Radical Initiated Polymerization of *p*-styrenesulfonate on Graphitic Carbon Nitride for Interconnected Water Networks in Short-Side-Chain PFSA Membranes for Low-Humidity Hydrogen Fuel Cells

Maniprakundil Neeshma[a,b], Punnappadam Rajan Suraj[a,b], Baskaran Mohan Dass[a], Santoshkumar D Bhat[a,b,*]

[a]CSIR-Central Electrochemical Research Institute-Madras Unit, CSIR Madras Complex, Chennai-600113, India

[b]Academy of Scientific and Innovative Research (AcSIR), Ghaziabad- 201002, India.

Correspondence: sdbhat@cecri.res.in

SUPPORTING INFORMATION

Materials

Melamine (Acros Organics), hydrogen peroxide (30 v/v%, Thermo Fischer Scientific), Sodium p-styrene sulfonate hydrate (TCI Chemicals), Potassium persulphate (Merck), DMAc (SRL Chemicals), Hydrochloric acid (SRL Chemicals), Deionized (DI) water with a resistivity of 18.2 MΩ·cm at 25°C was obtained from a Millipore Milli-Q® purification system (MilliporeSigma, USA) and was used for sample washing, solution preparation, membrane pretreatment etc.

Material characterization

Powder X-ray diffraction (XRD) data of CN and PSSCN were acquired using a Bruker Advance D8 X-ray diffractometer with Cu-Kα (λ = 1.5418 Å) radiation to see any structural and phase changes. X-ray photoelectron spectroscopy (XPS) was performed with an ESCALAB 250xi spectrometer, equipped with an XR6 micro-focused monochromator X-ray source (Al-Kα), for chemical state analysis. Scanning electron microscopy (SEM) images were recorded using a Vega3 electron microscope to observe the microstructure of CN and PSSCN. Fourier transform infrared spectroscopy (FTIR) was conducted using an IRSpirit (Shimadzu Pte. Ltd.) in the range of 4000-400 cm⁻¹ to analyze chemical structure details. Mechanical properties of the membranes were assessed using a universal testing machine (UTM, Tinius Olsen, H5KL) measuring tensile stress (MPa) and elongation at break (%). Thermal degradation profiles of the samples were examined by Thermogravimetric analysis (TGA, SDT Q600, TA instruments).

Water uptake, swelling ratio and Ion Exchange Capacity (IEC) measurement

The water retention ability of the membrane is evaluated by measuring its water uptake (WU). Initially, the membrane sample is dried in a vacuum oven at 80 °C for 12 hours, and its dry weight is recorded. Subsequently, the sample is submerged in deionized water for 24 hours in a sorption chamber to reach equilibrium, and the final weight is determined. Water uptake is then calculated using the following formula.

$$WU(\%) = \frac{Wwet - Wdry}{Wdry} \times 100 \dots\dots\dots\dots\dots\dots\dots\dots (S1)$$

W_{wet} and W_{dry} represent wet and dry weight of the membrane respectively.

The dimensional swelling ratio (SR) provides insight into how much the membrane expands in size when equilibrated with water. During the water uptake measurement, the dimensions of the membranes were recorded alongside their weight. The swelling ratio is calculated using the following formula,

$$SR(\%) = \frac{Lwet - Ldry}{Ldry} \times 100 \ldots\ldots\ldots\ldots\ldots\ldots\ldots\ldots (S2)$$

L_{wet} and L_{dry} represent wet and dry length of the membrane respectively.

To determine the ion exchange capacity (IEC) of the membrane, it was soaked in 50 ml of 0.01 M NaCl for 24 hours. Afterward, 10 ml of the resulting solution was titrated with 0.1 M NaOH. The ion exchange capacity is then calculated using the following relation[5].

$$IEC(meq/g) = \frac{(B - P) \times 0.01 \times 5}{Wdry} \ldots\ldots\ldots\ldots\ldots\ldots\ldots\ldots.. (S3)$$

B: Amount of NaOH required to neutralize the blank solution

P: Amount of NaOH required to neutralize the membrane-soaked solution.

0.01: Molarity of NaOH

5: Factor corresponding to the ratio of amount of NaCl used to soak the membrane to the amount used for titration

W_{dry}: Dry weight of the membrane

Proton conductivity measurement of membranes and PSSCN

The Electrochemical Impedance Spectra (EIS, Biologic SP-150) of the membrane samples were obtained at varying temperatures (30-90 °C) and relative humidities (30-100% RH) to realize the Ohmic resistance by keeping the sample in a controlled temperature and humidity chamber (Espec, SH-242). In-plane conductivity of the membrane samples was carried out using a four-probe BekkTech conductivity cell wherein the high-frequency resistance (HFR) of the membranes was measured via frequency sweep from 1 MHz to 1 Hz with an amplitude of 10 mV. From the HFR value, membrane proton conductivity was measured using the equation,

$$\sigma = L/RA\ldots\ldots\ldots\ldots\ldots\ldots\ldots (S4)$$

Where σ is the conductivity of the sample (S cm^{-1}), L is the length between voltage separating probes (0.425 cm), R and A denote the real-impedance axis intercept of the Nyquist plot and area of the membrane sample respectively.

PSSCN was subjected to proton conductivity measurement using the same technique at 95 % RH by keeping the sample in pellet form in a two-probe setup with a thickness of 0.02 cm and a radius of 0.5 cm. The proton conductivity was obtained from the Nyquist plot using equation S4, where L is the thickness of the sample pellet and A cross-sectional area of the pellet.

The activation energy for ionic transport was also determined from the temperature-dependent conductivity data, fitted to an Arrhenius plot using Equation S5[7].

$$\ln \sigma = \ln\sigma0 - {Ea}/{RT} \ldots\ldots\ldots\ldots\ldots\ldots\ldots \text{(S5)}$$

σ0: pre-exponential factor

R: Universal gas constant

T: Temperature in K

Ex-situ membrane oxidative stability test

Fenton's test was employed to assess the oxidative stability of the membranes. The membranes were immersed in Fenton's reagent (3% H_2O_2 and 4 ppm Fe^{2+}) at 80°C for 24 hours . The initial dry weights of the samples were recorded, and the weight changes were monitored to determine the degradation rate. The membrane samples were thoroughly washed with DI water and dried at 60°C before weighing[2].

MEA fabrication and fuel cell test:

Catalyst-coated membranes (CCM) were fabricated by hot-pressing decal-coated catalyst layers at 140°C under a pressure of 2 kg m^{-2} for 3 minutes, with a platinum (Pt) loading of 0.3 mg cm^{-2} on both the anode and cathode. The membrane electrode assembly (MEA) was then prepared by sandwiching the CCM between commercial gas diffusion layers (GDL-BC36, Alfa Aesar GmbH & Co. KG, Germany) and assembled in a commercial single-cell fixture (Fuel Cell Technologies Inc., USA) with an active area of 5 cm^2 using an applied torque of 4.5 Nm. Graphite monopolar plates with serpentine flow fields were employed to distribute fuel and oxidant, along with current collector plates and end plates. Single-cell performance evaluation, including polarization studies, was conducted using a fuel cell test station (Fuel Cell Technologies Inc., USA) under no applied back pressure. During testing, a stoichiometric flow ratio of 1.3:3 for high-purity H_2 and O_2 was maintained at the anode and cathode, respectively, throughout both the conditioning and polarization studies. Polarization tests were performed at 65°C under three different relative humidity (RH) conditions. Before collecting each polarization dataset, the MEA was conditioned for 6 hours using an electronic load model (N3300A) from the fuel cell test station. The performance of the composite membranes was analyzed and compared to MEAs fabricated with pristine Aquivion membranes, ensuring that all other parameters remained consistent to allow for a valid comparison of data[7].

MEA durability and H_2 crossover studies

The chemical stability of recast pristine Aquivion (AQ) and nanocomposite membrane (AQPC 1)-based MEAs was evaluated under open-circuit voltage (OCV) hold conditions at a cell temperature of 85°C and 30% relative humidity (RH). A stress test was performed using an electronic load model (N3306A) from the fuel cell test station following a slightly modified DoE accelerated stress protocol. The test ran for 100 hours, incorporating a start-up/shut-down cycle of 10 hours each day. During the AST, high-purity hydrogen and air were supplied to the anode and cathode at flow rates of 100 mL min^{-1} and 200 mL min^{-1}, respectively. Polarization curves were recorded at dry gas, 30% and 100% RH of H_2 and O_2, and a temperature of 65°C, with no applied backpressure to assess performance degradation before and after the AST. Additionally, fuel permeability/hydrogen crossover through the membranes were measured using linear sweep voltammetry (LSV). This was conducted using a potentiostat (Parstat MC (PMC 2000A, Ametek scientific Instruments) in a fuel cell setup, with the cathode as the working electrode and the anode as both the reference and counter electrodes. LSV was performed over a potential range of 0.05 to 0.5 V at a scan rate of 10 mV s^{-1}, while maintaining a cell temperature of

65°C. 100% humidified H_2 and N_2 gases were supplied at 150 mL min^{-1} to the anode and cathode, respectively. Prior to LSV measurement, the cell was conditioned for 1 hour under H_2 and N_2 conditions, and cyclic voltammetry (CV) was performed for 30 cycles to further evaluate the electrochemical behavior of the membranes[7].
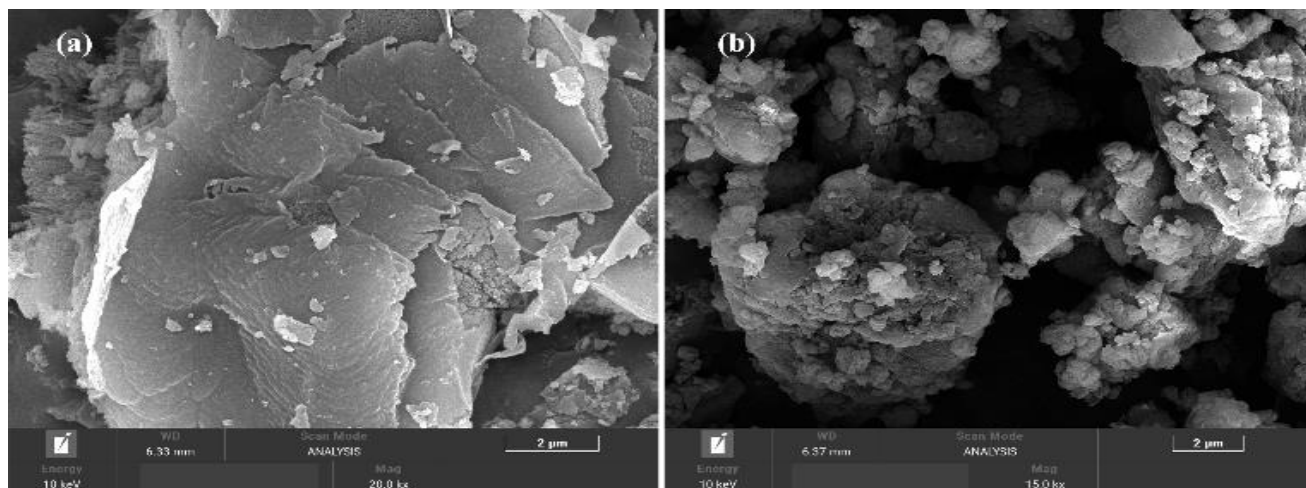
Figure S1. FESEM images of (a) CN and (b) PSSCN revealing the morphological changes after the radical initiated polymerisation of PSSA on CN.
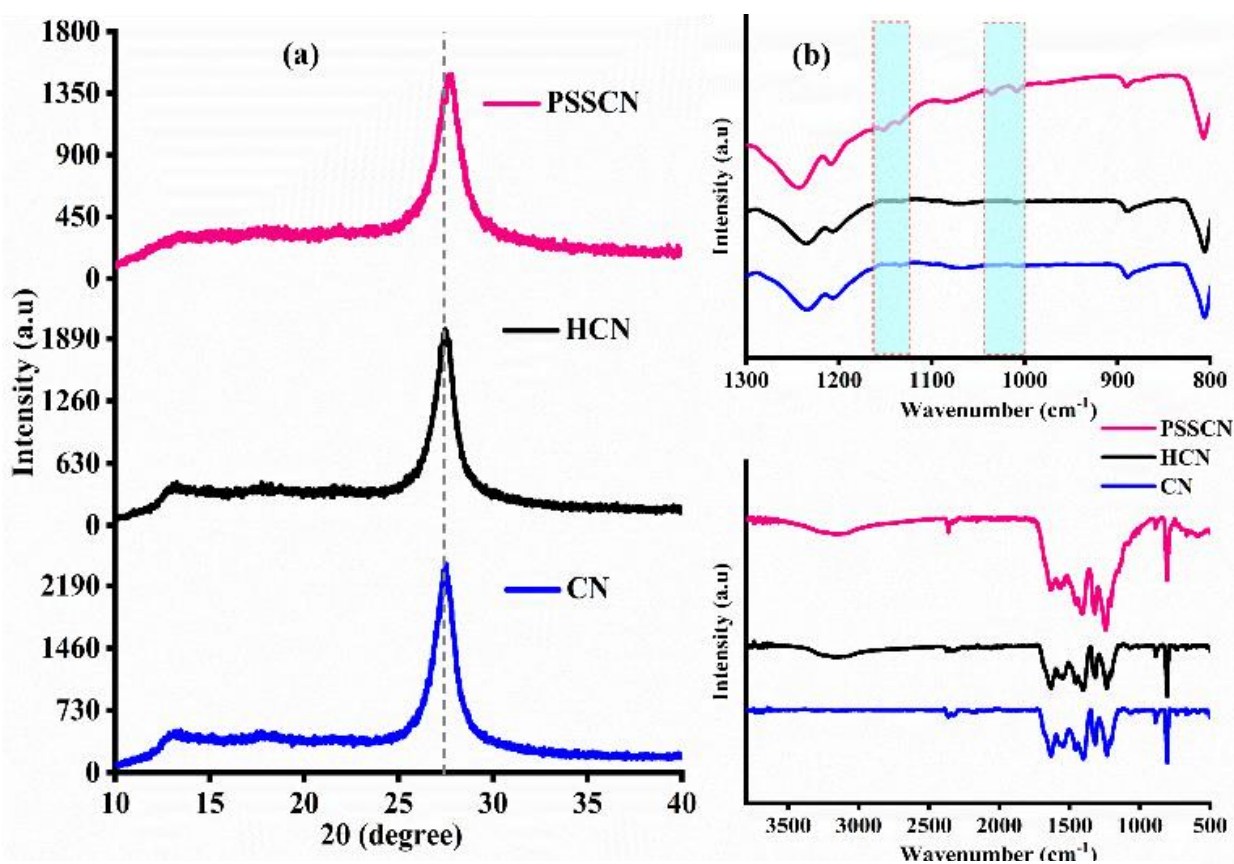
Figure S2. (a) XRD patterns and (b) FTIR spectra of CN, HCN, PSSCN showing successful surface modifications upon H_2O_2 treatment and SS grafting on CN
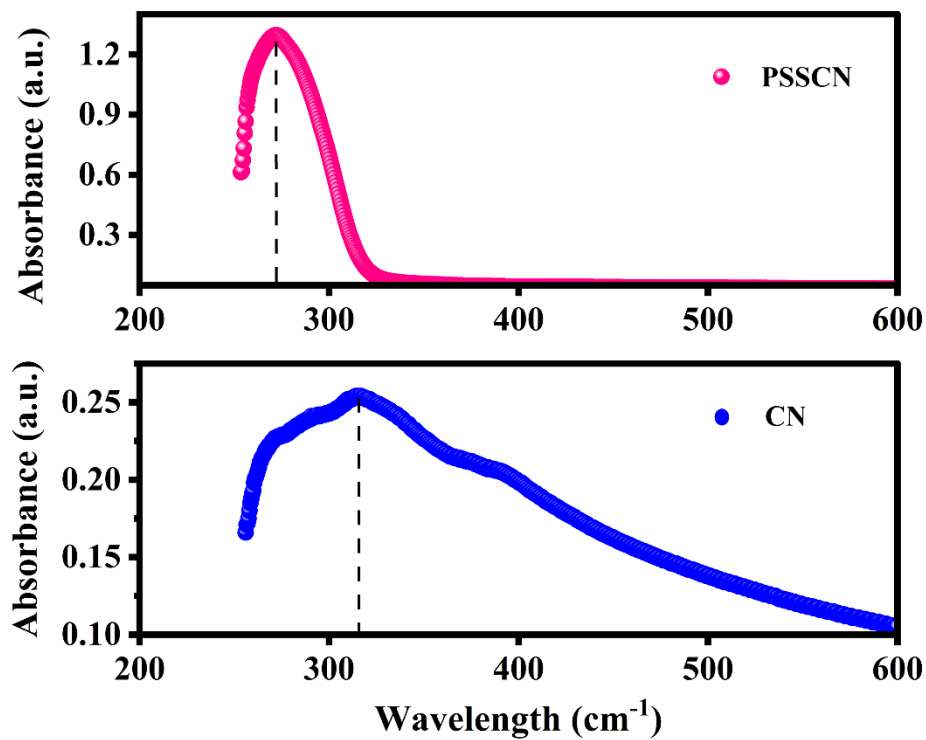
Figure S3. UV-Visible absorbance spectra of PSSCN and CN showing a blue shift in the absorbance peak of PSSCN towards 270 nm due to PSSA grafting.
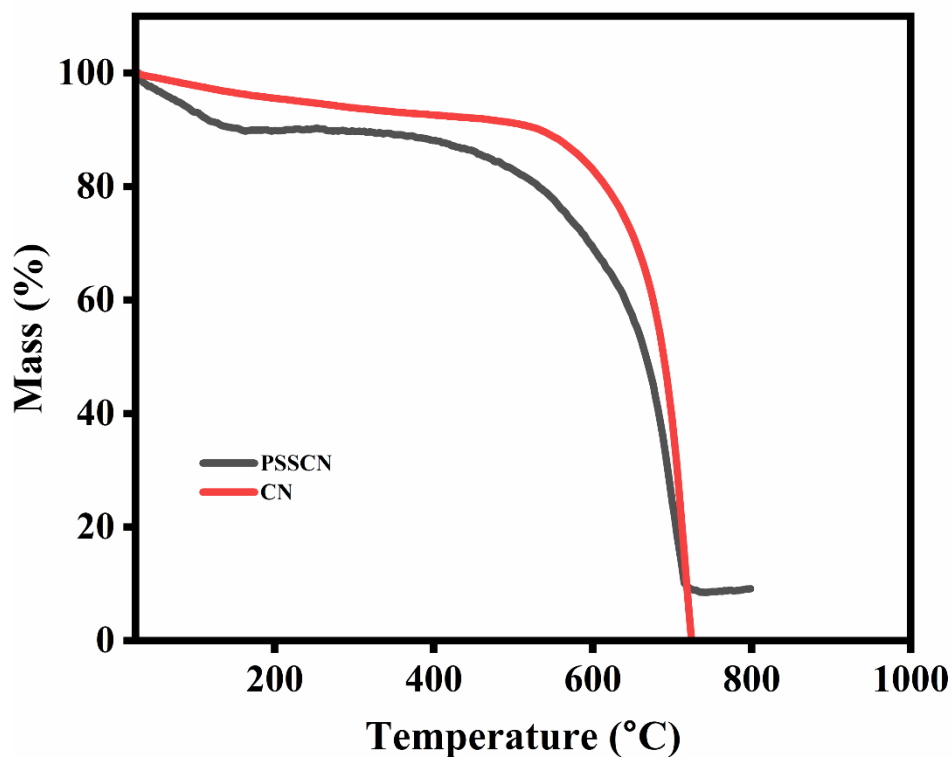
Figure S4. TGA curves of PSSCN and CN, showing an earlier onset of degradation for PSSCN, indicating PSSA grafting.
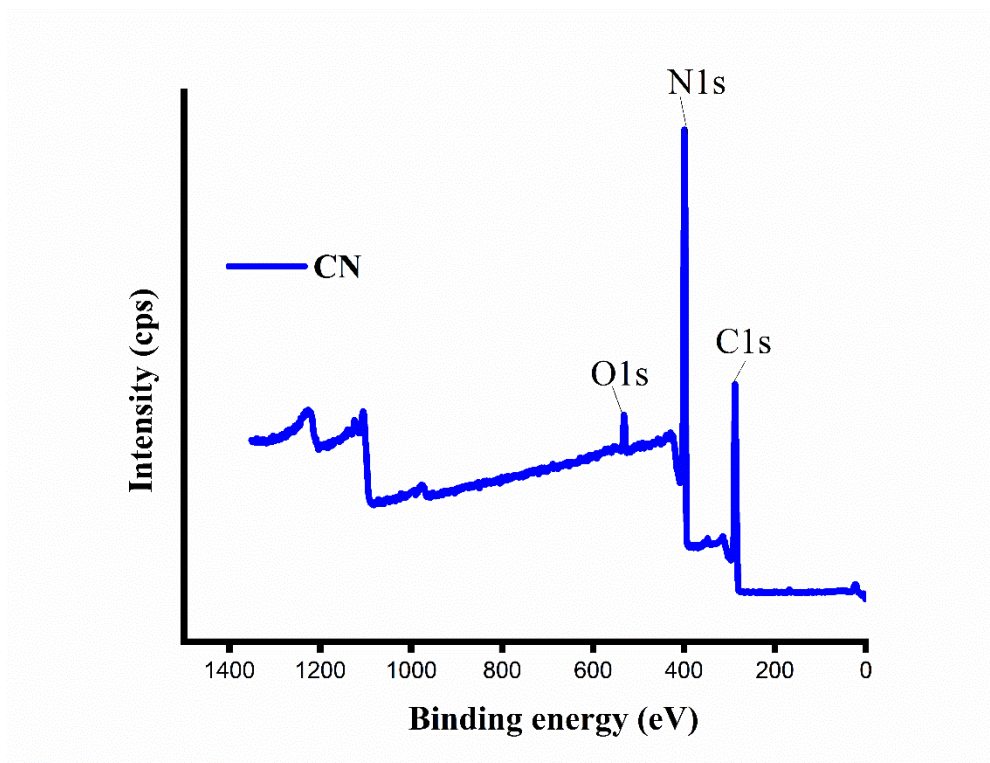
Figure S5. XPS survey spectra of CN
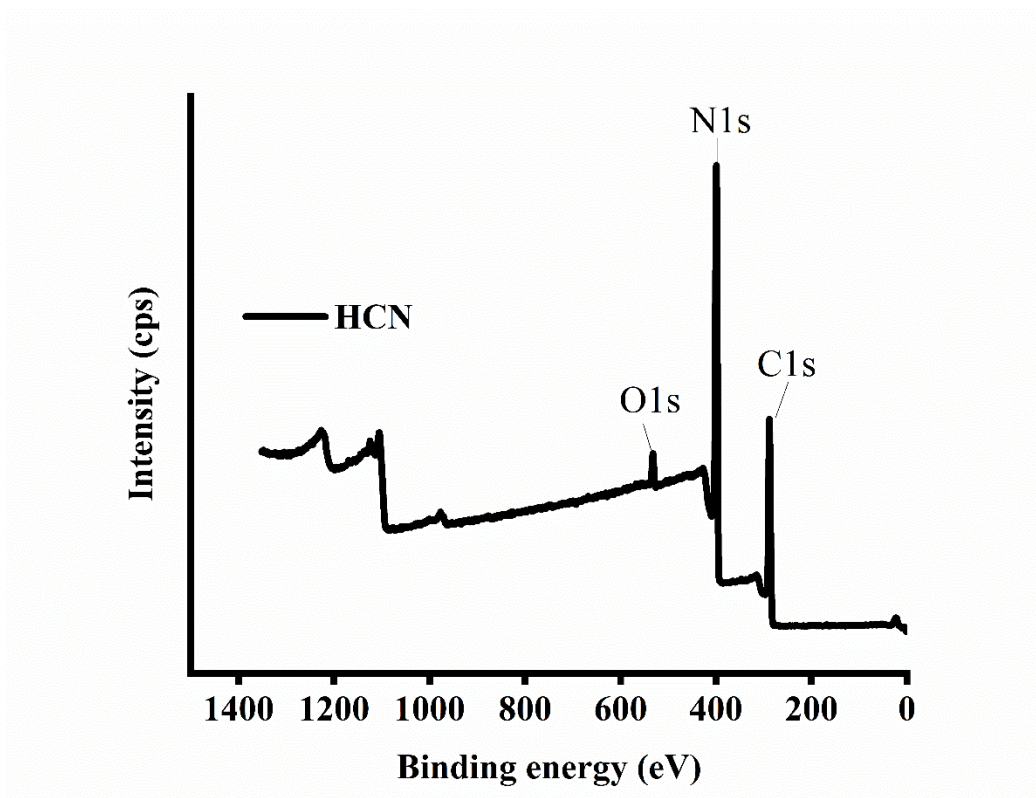
Figure S6. XPS survey spectra of HCN
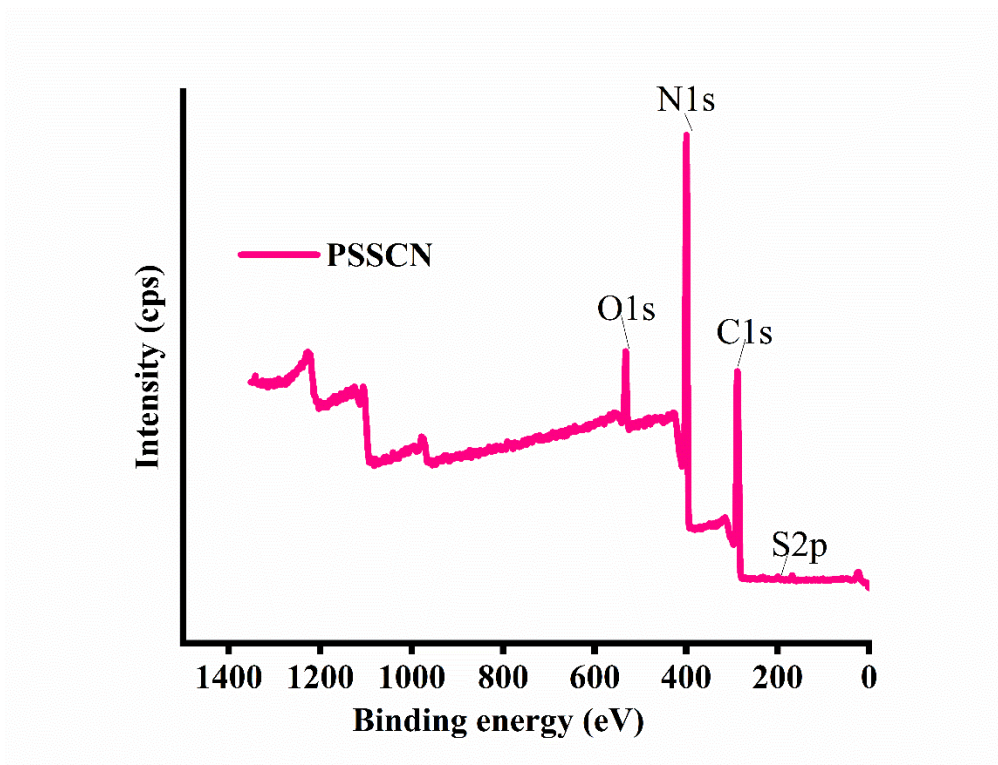
Figure S7. XPS survey spectra of PSSCN
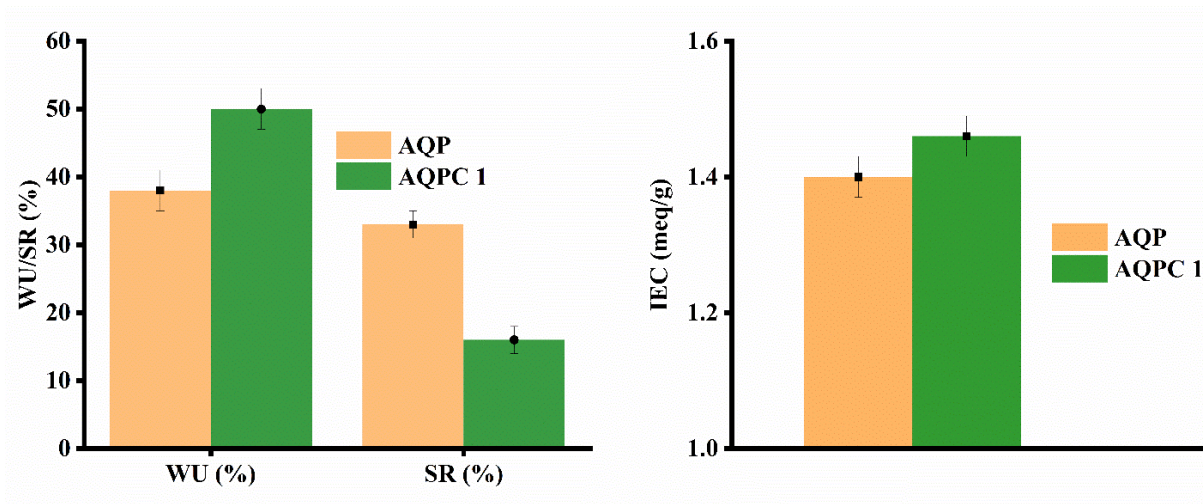
Figure S8. Water uptake (WU %) Swelling ratio (SR %) and IEC (meq/g) of AQP and AQPC 1 membranes
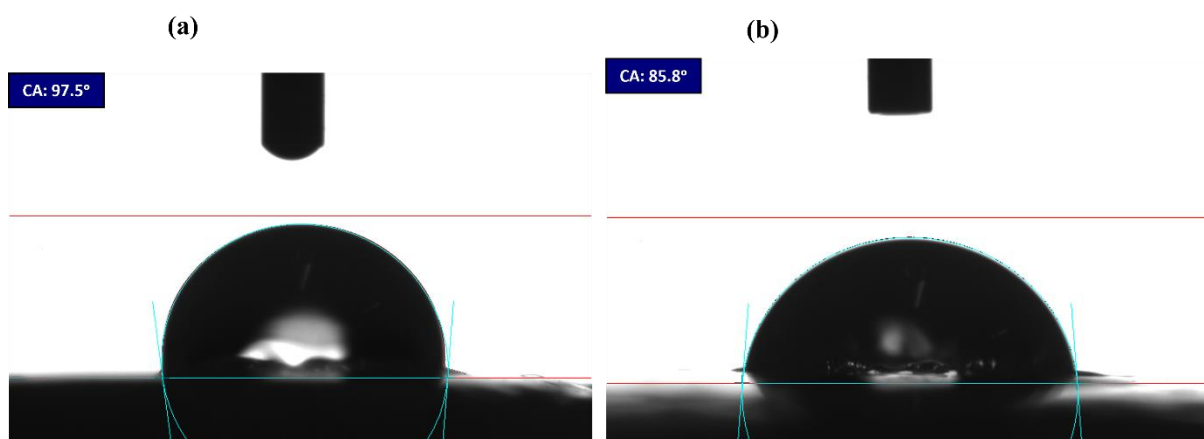
Figure S9. Contact angle measurements showing changes in wettability of AQP (a) after incorporation of PSSCN indicating increased hydrophilicity of AQPC 1 (b).
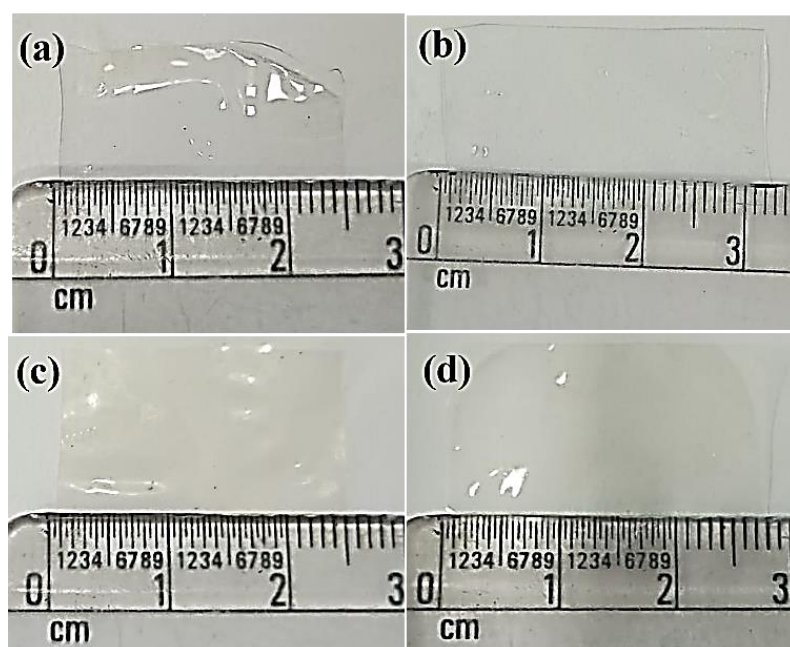
Figure S10. Dimensional changes of the AQP membrane (a, b) and AQPC 1 membrane (c, d) before and after equilibration in water
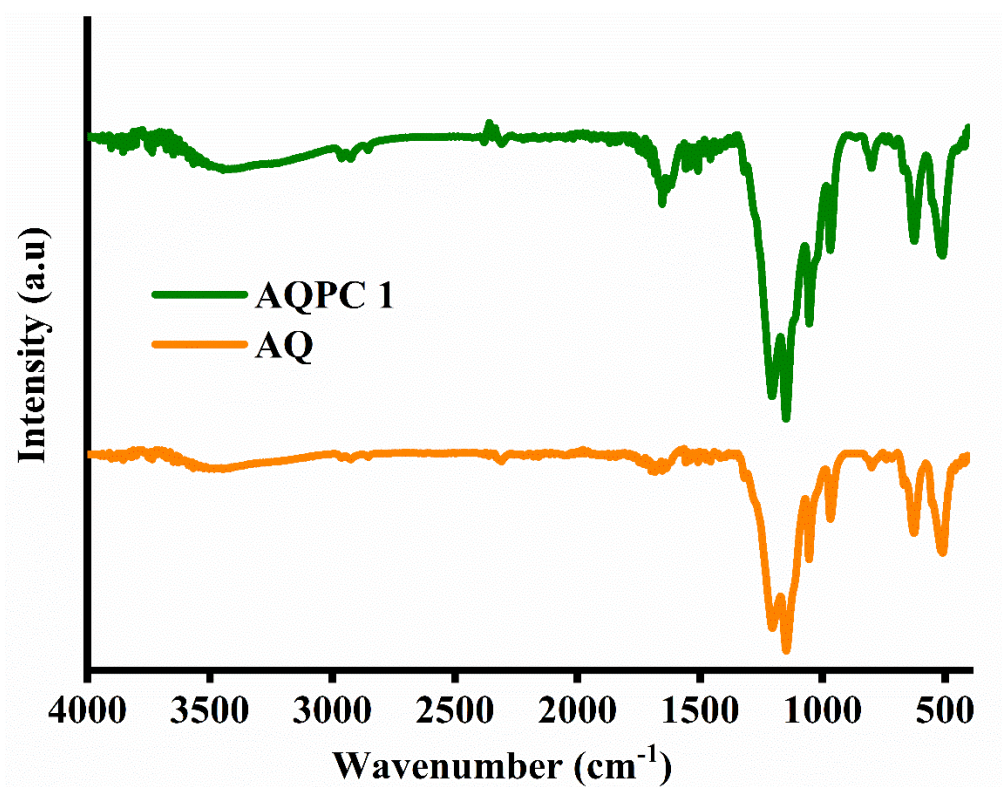
Figure S11. FTIR-ATR spectra of AQ and AQPC 1 membranes
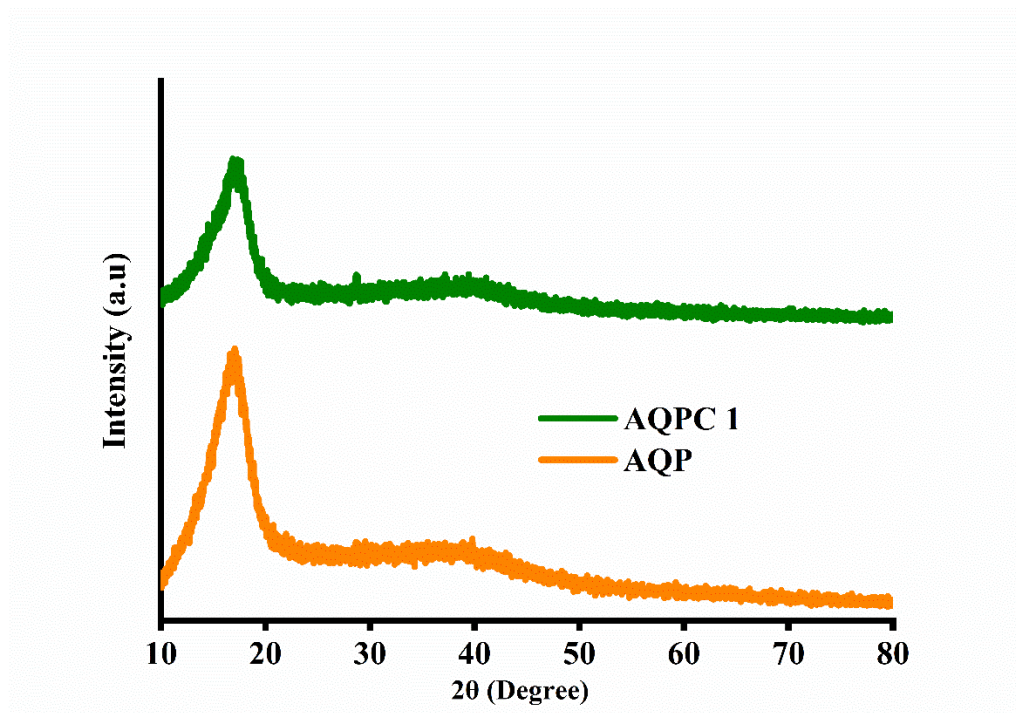
Figure S12. XRD spectra of AQP and AQPC 1 membranes
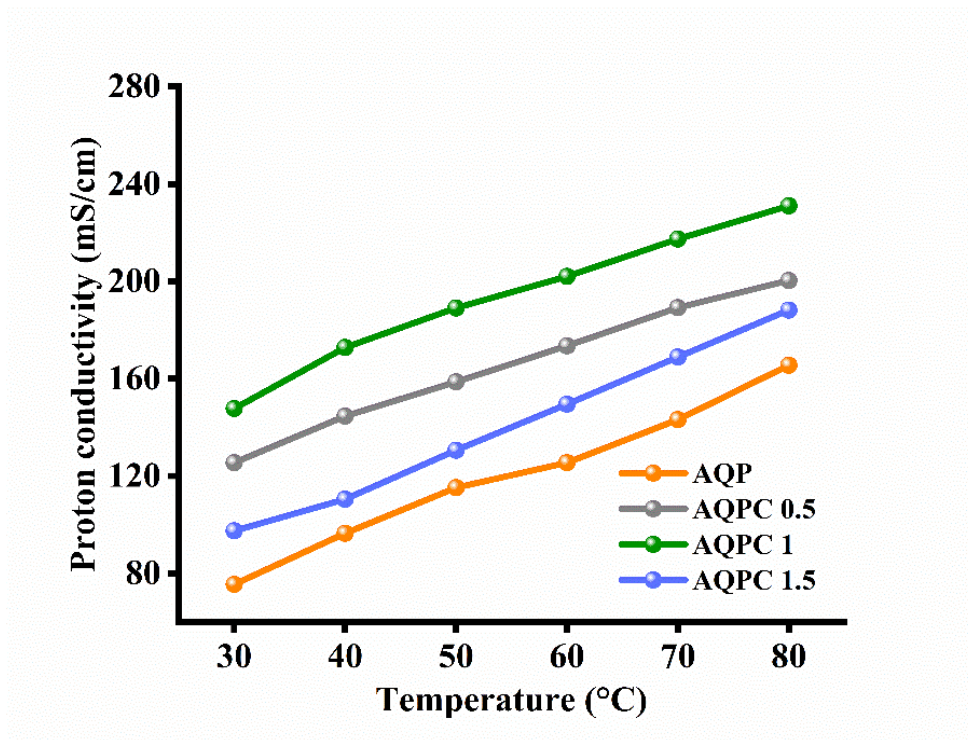
Figure S13. Comparison of proton conductivities of AQPC membranes with different weight percentages of PSSCN
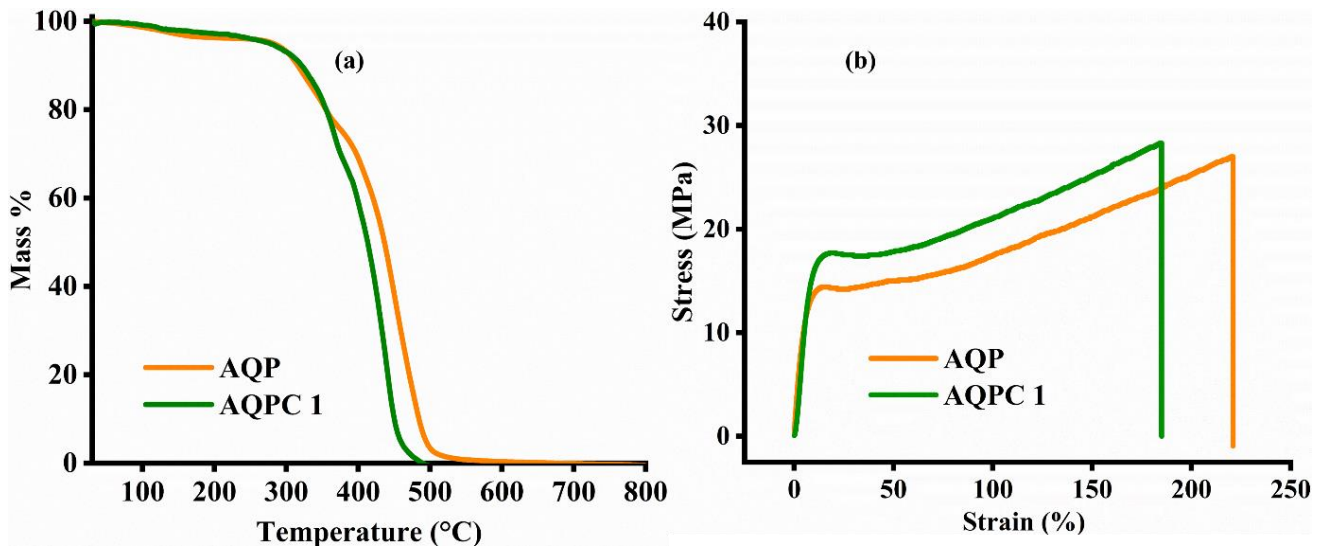
Figure S14. (a) Thermogravimetric analysis showing thermal stability and degradation profiles of membranes (b) Stress-strain curve showing mechanical stability, elasticity and ultimate strength of membranes
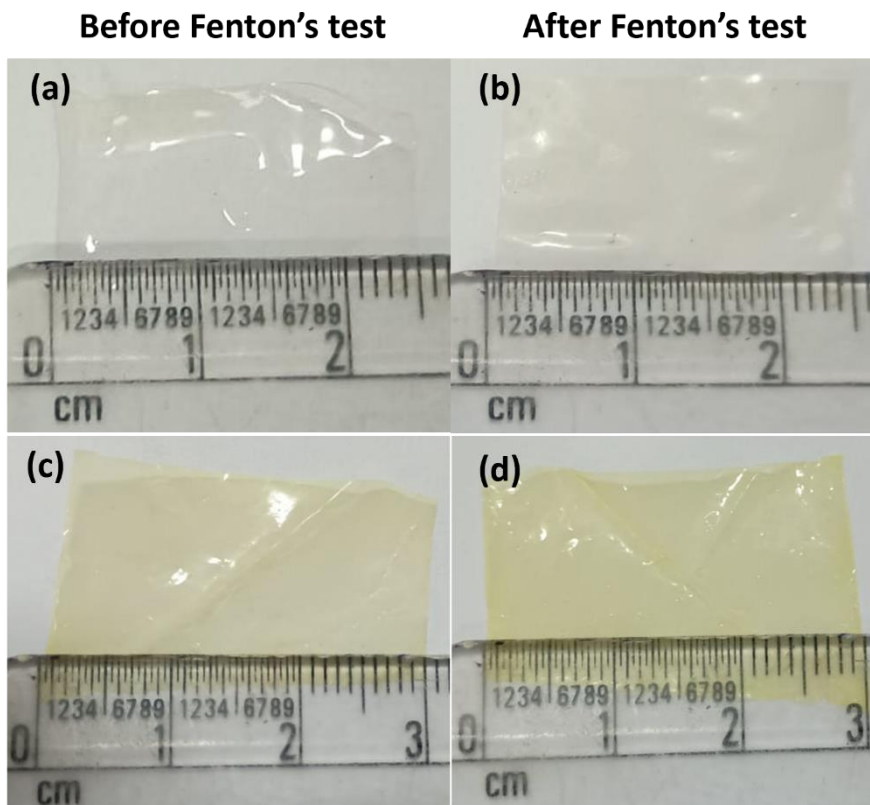
Figure S15. AQP membrane (a) before and (b) after Fenton's test; AQPC 1 membrane (c) before and (d) after Fenton's test.
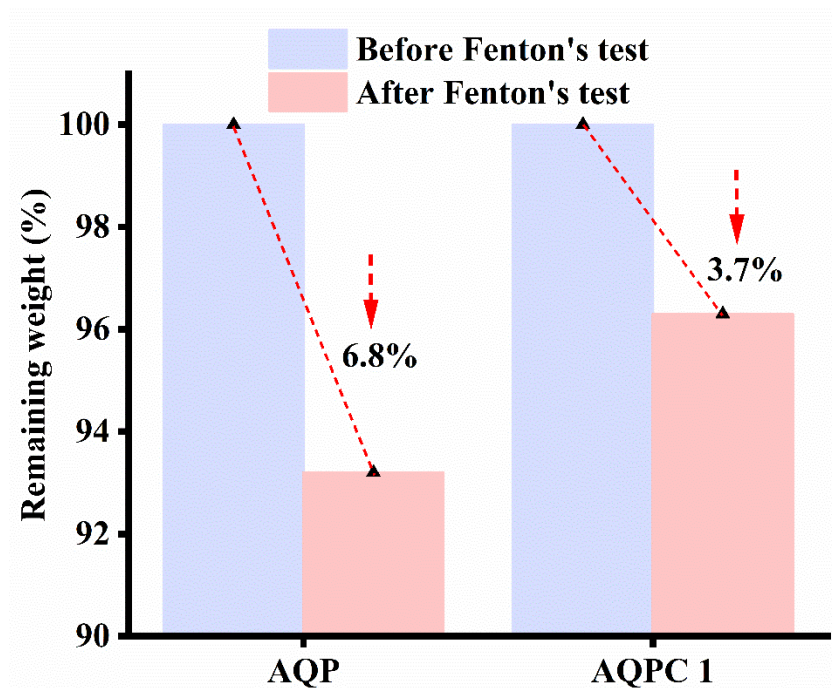
Figure S16. Weight degradation of membranes after exposure to Fenton's reagent for 24 hours at 80 °C
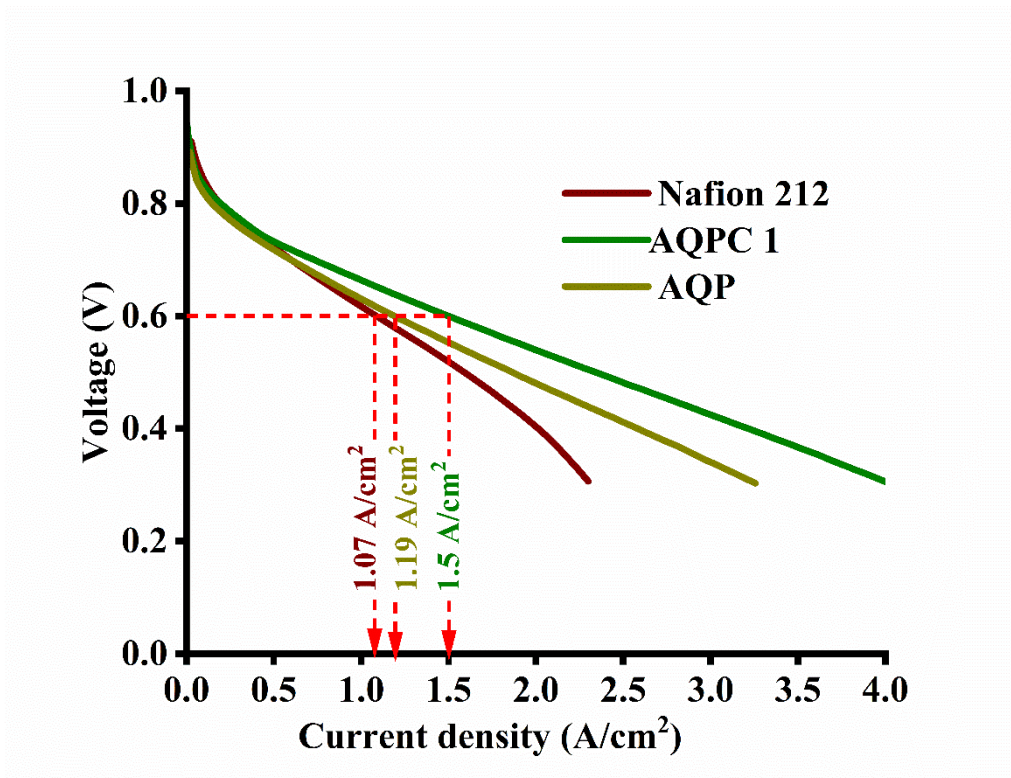
Figure S17. Fuel cell performance comparison of AQPC1 membrane with AQP and Nafion 212 commercial membrane
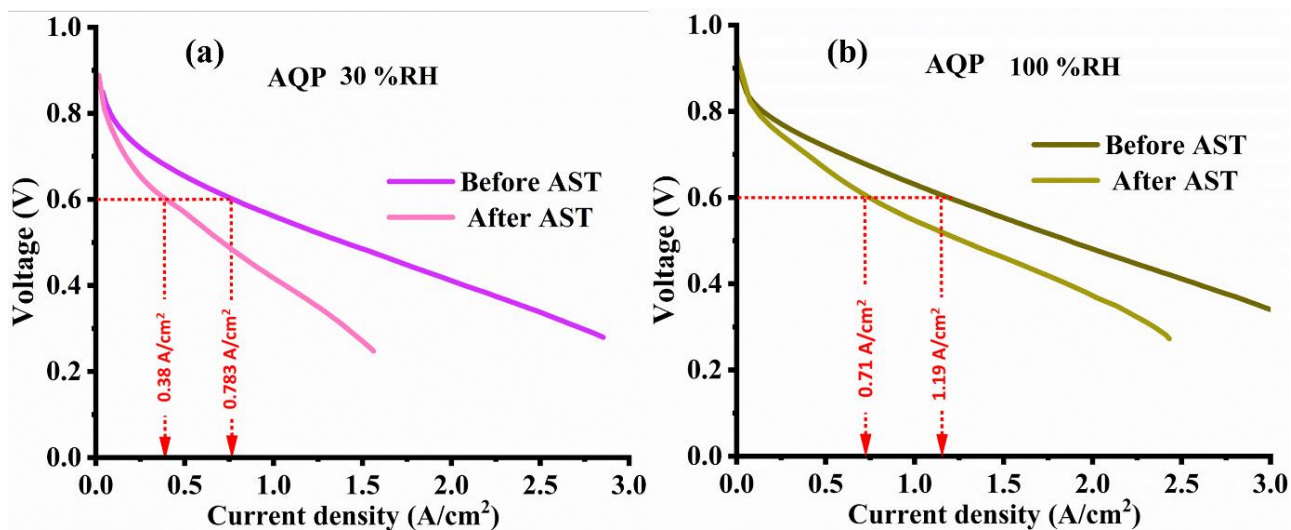
Figure S18. Comparison of the fuel cell performance of Aquivion membrane before and after AST
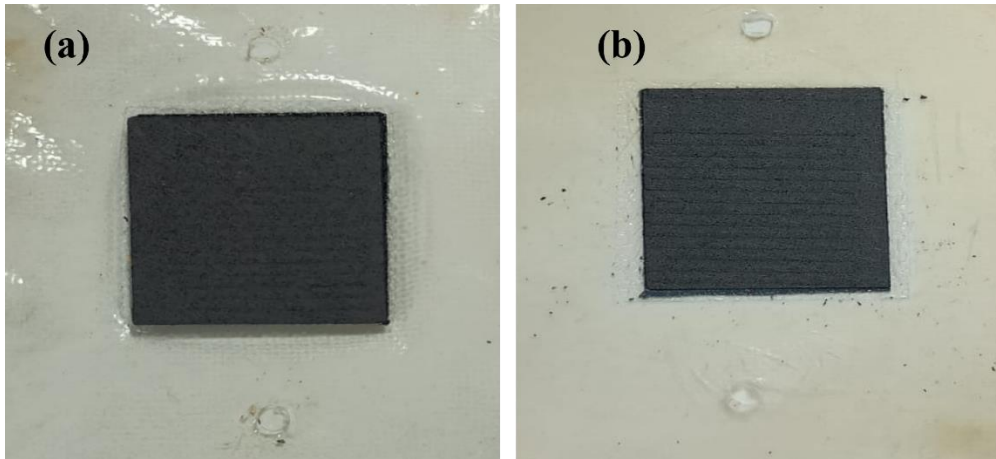
Figure S19. MEAs after 100 hours of AST (a) AQP (b) AQPC 1
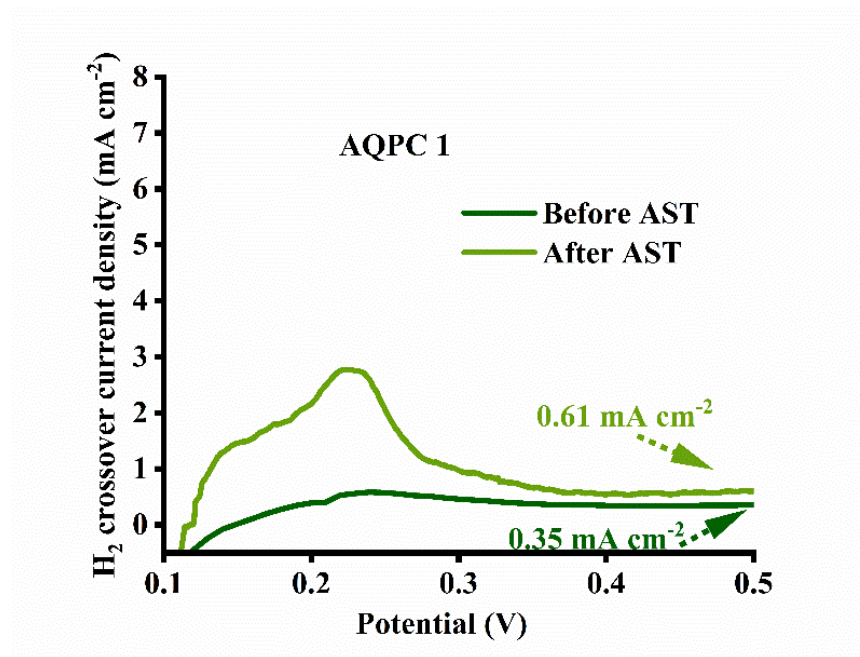
Figure S20. Hydrogen crossover current densities of AQPC 1 membrane at 100% RH and 65°C before and after AST

Table S1. Comparative analysis of filler-incorporated PEMs, highlighting equivalent weight of the Aquivion ionomer, proton conductivity and peak power density.

Filler	Equivalent Weight of SSC PFSA ionomer (g/mol)	Conductivity (mS/cm)	Peak Power Density (W/cm²)	Reference
HPA functionalized on Zeolite Imidazolate Framework-67	790	90 (80 °C 30% RH)	0.72	1
Functionalized ceria nanoparticles	790	168 (90 °C 95% RH)	1.6	2
$(Co(bpy)(H_2O)_4.(H_2O)_{1.5}$	790	50.6 (RT 100% RH)	0.45	3
$[(Me_2NH_2)_3(SO_4)]_2[Zn_2(ox)_3]\}n$	790	34.9 (25 °C 100% RH)	0.497	4
Polystyrene sulfonic acid grafted cup-stacked carbon nanofiber	720	189.7 (80 °C 95% RH)	1.4	5
Phosphonic acid-functionalized mesoporous silica nanoparticles	--	136 (80 °C 90% RH	1.5	6
Tungsten semi-carbide	720	190 (80 °C 95% RH)	1.38	7
Fluoroalkyl Zirconium Phosphate	700	430 (110 °C 95% RH)	0.34	8
ePTFE	--	180 (120 °C 100% RH)	--	9
Modified halloysite nanotubes	830	280 (90 °C 90% RH)	--	10
Polystyrene sulfonic acid grafted carbon nitride	**720**	**230 (80 °C 95% RH)**	**1.3**	**Present work**

References

1. Ryu, G. Y., Jae, H., Kim, K. J., Kim, H., Lee, S., Jeon, Y., Roh, D., Chi, W. S. ACS Appl. Energy Mater. 2023, 6, 4283–4296.
2. B. M. Dass, M. Neeshma, S. M. Unni, V. M. Dhavale, D. Prabhakaran and S. D. Bhat, ACS Appl. Polym. Mater., 2024, 6, 11691-11705.
3. Paul, S., Choi, SJ., Kim, H.J. Ionics 2021, 27, 1653–1666.
4. Paul, S., Choi, S., Kim, H.J., Energy Fuels 2020, 34, 10067–10077.
5. M. Neeshma, P. Dhanasekaran, S. M. Unni and S. D. Bhat, J. Memb. Sci., 2023, 668, 121240.
6. Huang, H., Xu, S., Zhang, L., Fan, J., Li, H., Wang, H. Sustainable Energy Fuels, 2021, 5, 230.
7. M. Neeshma and S. D. Bhat, ACS Appl. Mater. Interfaces, 2023, 15, 53881–53890.
8. Donnadio, A., Pica, M., Subianto, S., Jones, D. J., Cojocaru, P., Casciola, M. ChemSusChem 2014, 7, 2176–2184.
9. Xiao, P., Li, J., Chen, R., Wang, R., Pan, M., Tang, H., Int. J. Hydrogen Energy 2014, 39, 15948–15955.
10. Woo, S.H., Taguet, A., Otazaghine, B. J Mater Sci., 2021,56, 13108–13127.